Availableonlinewww.jocpr.com

Journal of Chemical and Pharmaceutical Research, 2020, 12(9): 17-28

Research Article

ISSN: 0975-7384
CODEN(USA): JCPRC5

Coordination Chemistry of Colored Food Additive Red 2G

Mamdouh S Masoud[1], Alaa E Alib[2] and Ragab Y Sharafc[3]

[1]Chemistry Department, Faculty of Science, Alexandria University, Alexandria, Egypt

[2]Chemistry Department, Faculty of Science, Damanhur University, Damanhour, Egypt

[3]Regional Joint Lab, Al Beheira Governorate, Ministry of Health, Damanhour, Egypt

---

ABSTRACT

Food additives are any substance not normally considered as a food by itself and not normally used as a typical ingredient of the food, not required nutritive value. Metal complexes of these colored food additive Red 2G is synthesized. The ligand is azo compound, elemental analysis of the prepared metal complexes, structural investigation of the complexes based on: Infrared, electronic spectra, and magnetic susceptibility, ESR study of copper complex was investigated. All complexes are of octahedral geometry. The thermal properties of the studied complexes were examined.

Keywords: Coordination chemistry; Metal complexes; Red 2G; Spectral; Thermal analysis

---

INTRODUCTION

Food colorings are tested for safety by various bodies around the world and sometimes different bodies have different views on food color safety. In the United States, FD & C numbers which generally indicated that the FDA has approved the colorant for use in foods, drugs and cosmetics are given to approved synthetic food dyes that do not exist. Masoud et al. gave different view on food color safety through the interaction between colored food additives and heavy metal ions to form water insoluble complexes in which may be leads to accumulation in human bodies (Figure 1).

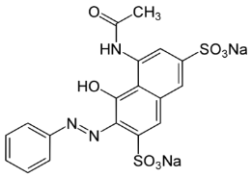

Figure 1. Red 2G

EXPERIMENTAL

Mono metal-ligand (Red 2G) complexes were prepared in a similar manner. The inorganic salts [Cr(III), Mn(II), Fe(III), Co(II), Ni(II), Cu(II), Zn(II) and Cd(II) as chlorides] were dissolved in 10 mL de-ionized water. Each ligand was dissolved in de-ionized water and ethanol by ratio (2:1). The molar amount of the metal chloride salt was mixed with the calculated amount of the ligand in the molar ratios (1:1).The reaction mixture was refluxed for about 5 min then left over-night, where the precipitated complexes were separated by filtration, then washed several times with a mixture of CH_3CH_2OH-H_2O and dried in a vacuum desiccator over anhydrous $CaCl_2$[1].

RESULTS AND DISCUSSION

IR of Red 2G and its complexes

The IR spectra of Red 2G, gave bands at 3431, 2925, 1608,1486, 1384, 1127, 1051 and 616 cm^{-1} due to υ_{OH}, υ_{C-H}, $\upsilon_{C=C}$, υ_{C-C}, $\upsilon_{N=N}$, υ_{C-N}, υ_{S-O} and $\upsilon_{N=N}$, respectively. These bands are affected on complexation, due to electron withdrawing properties of the metal ions. However, the metal complexes gave υ_{OH} bands spectra, (Table 1), at 3437, 3377, 3423, 3402, 3401, 3393, 3470 and 3539 cm^{-1} for Cr, Mn, Fe, Co, Ni, Cu, Zn and Cd complexes, respectively. The higher shift is observed for the hard metals.

The band due to υ_{C-H} of the ligand is unchanged in Cu complex and absent in Mn, Fe, Co, Ni, Zn and Cd complexes. However,$\upsilon_{C=C}$ bands ranged in complexes from 1608-1614 cm^{-1}, to reflect that the band is affected in all complexes by same manner. Similar behavior of υ_{C-C} is observed [2-4]. The bands due to $\upsilon_{N=N}$ at 1486, 1484, 1487, 1487, 1487, 1488, 1489 and 1488 cm^{-1} for Cr, Mn, Fe, Co, Ni, Cu, Zn and Cd complexes, respectively, (Table 1), where N=N group is involved on complexation.

The υ_{C-N} band appeared at 1177, 1174, 1181, 1178, 1183, 1185, 1182 and 1127 cm^{-1} for Cr, Mn, Fe, Co, Ni, Cu, Zn and Cd complexes, respectively. The shifted range reflects that this band is affected on complexation. The band responsible for υ_{S-O} appeared at about 1049, 1048, 1049, 1049, 1051, 1050, 1052 and 1053 cm^{-1} for Cr, Mn, Fe, Co, Ni, Cu, Zn and Cd complexes, respectively.

The small change reflects that this band is slightly affected on complexation. The $\upsilon_{N=N}$ band at 656, 650, 655, 653, 655, 649, 652 and 615 cm^{-1} for Cr, Mn, Fe, Co, Ni, Cu, Zn and Cd complexes, respectively indicating that the azo group is contributed on complexation.

New bands appeared at ~455 and ~550 cm^{-1} due to υ_{M-O} and υ_{M-N}, respectively. So, in all complexes the metal ion combined with Red 2G through the azo group and the O-hydoroxy of the naphthalene moiety resulting in formation of a stable six membered ring. Also, all the prepared complexes contain water molecules [5-9].

Electronic absorption spectra of Red 2G and its complexes

Red 2G free ligand, (Figure 1), gave three main bands. Band at 220 nm, due to $n\rightarrow\pi^*$ electronic transition of the OH group, presents at naphthalene ring, so the azo group is electronically shifted towards the phenyl ring rather than the naphthalene rings by the donating character of the hydoroxy group.

Table 1. Fundamental infrared spectral bands (cm^{-1}) of Red 2G and its complexes.

Complexes	Infrared spectral bands									
	υ_{OH}	υ_{X-H}	$\upsilon_{X=X}$	υ_{X-X}	$\upsilon_{N=N}$	υ_{X-N}	$\upsilon_{\Sigma-O}$	$\delta_{N=N}$	υ_{M-O}	υ_{M-N}
Red 2G (HL)	3431	2925	1608	1535	1486	1127	1051	644	-	-
[CrL $(OH)_2(H_2O)_2$]	3437	2925	1611	1536	1446	1173	1049	656	523	477
[Mn LOH$(H_2O)_3$]	3377	2927	1608	1536	1454	1174	1048	653	528	451
[FeL $(OH)_2(H_2O)_2$]	3423	2920	1608	1535	1437	1181	1049	655	520	480
[Co LOH$(H_2O)_3$]	3402	2926	1608	1537	1472	1178	1049	653	510	455
[Ni L OH$(H_2O)_3$]	3401	2926	1607	1538	1457	1183	1051	655	529	453
[Cu L OH$(H_2O)_3$]	3393	2925	1607	1535	1461	1185	1050	649	500	456
[Zn L OH$(H_2O)_3$]	3440	2927	1609	1535	1439	1182	1052	652	532	455
[Cd L OH$(H_2O)_3$]	3539	2930	1614	1536	1448	1172	1053	615	530	455

The band at 420 nm is due to $\pi \rightarrow \pi^*$ electronic transition of the azo group, where it may interact with the phenyl or naphthalene moities of the ligand through the electron with drawing character of –SO3H and –NH– groups. Band at 490 nm is due to n $n \rightarrow \pi^*$ electronic transition.

For Red 2G chromium complex, d^3, the spectrum gave two peaks at 440 and 560 nm, due to $^4A_2 \rightarrow ^4T_1$ (F) and $^4A_2 \rightarrow ^4T_2$, transitions, respectively, indicating octahedral structure [10]. The room temperature magnetic moment value is 3.60 BM indicating the high spin nature, (Figure 2).

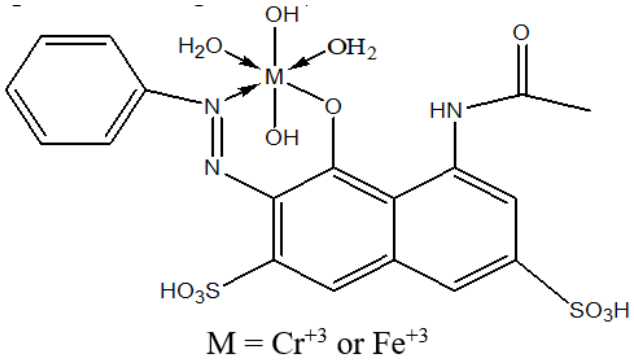

Figure 2. Structure of [Cr L $(OH)_2(H_2O)_2$] and [Fe L $(OH)_2(H_2O)_2$] complexes.

For Red 2G manganese complex, [MnLOH $(H_2O)_3$].$2H_2O$, gave two bands at 530 and 870 nm. The first band is assigned $^6A_{1g} \rightarrow {}^4T_{2g}$ transition and the last band is due to $^6A_{1g} \rightarrow {}^4T_{1g}$ transition. Its room temperature μ_{eff} value of 3.72 BM typified the existence of O_h configuration with sp^3d^2 hybridization, and bidentate nature of the organic compound and three water molecules in the inner sphere of the complex. The structure of the complex is given in Figure 3.

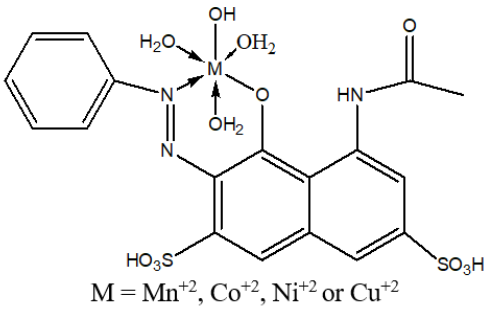

Figure 3. Structure of Mn^{+2}, Co^{+2}, Ni^{+2} or Cu^{+2} complexes of Red2G.

The electronic absorption spectra of the Red 2G iron-complex, $[FeLOH.(H_2O)_3]H_2O$ gave bands at 420, 470, 860 nm, These bands are due to CT ($t_{2g} \rightarrow \pi^*$) and CT ($\pi \rightarrow e_g$). Its room temperature μ_{eff} value of 5.40 B.M typified the existence of O_h configuration in high spin state with sp^3d^2 hybridization [11], figure 2. However, The Red 2G cobalt $[CoLOH(H_2O)_3]$complex, Figure 3, gave bands at 440 and 500 nm. The first band is of $^4T_{1g}(F) \rightarrow {}^4A_{2g}(P)$ and the second one assigned to $^4T_{1g}(F) \rightarrow {}^4T_{1g}(P)$ transition, its room temperature magnetic moment value of 5.91 BM typified the existence of the complex in O_h geometry with high spin nature [12]. However, the Red 2G Nickel $[NiLOH(H_2O)_3]$complex gave three bands at 440, 500 and 660 nm, are due to $^3A_{2g} \rightarrow {}^3T_{1g}$ (p), $^3A_{2g} \rightarrow {}^3T_{1g}$ (f) and $^3A_{2g} \rightarrow {}^3T_{2g}$, respectively. These bands indicate O_h structure with high spin nature [13]. The room temperature magnetic moment value is 2.77 BM reflecting the paramagnetic nature of the complex, with hyperdization of sp^3d^2. The structure of the complex is shown in Figure 3. The electronic absorption spectra of Red 2G copper $[CuLOH(H_2O)_3]$complex gave bands at 220, 440, 480 and 670 nm, due to d-d transition of a disoriented O_h structure [14-16]. The room temperature magnetic moment value is 1.92 BM, confirmed the high spin O_h structure, to assign the weak ligand nature of Red 2G. However, the electronic absorption spectra of Red 2G zinc complex gave three bands at 420, 472 and 544 nm, are assigned to charge transfer. Owing to the d^{10} configuration of Zn (II), the stereochemistry around metal ion in its complex is assumed to have Oh structure (Figure 4).

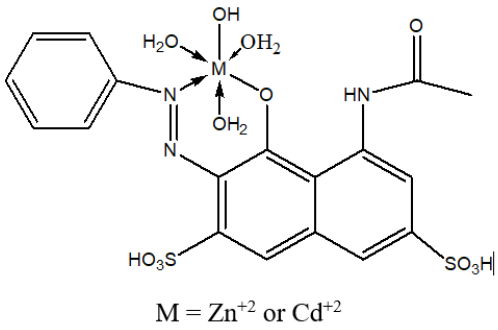

Figure 4. Structure of [Zn LOH $(H_2O)_3$]and [Cd LOH $(H_2O)_3$] complexes.

However, the cadmium complex gave three bands at 420, 460 and 550 nm, are assigned to charge transfer. The stereochemistry around metal ion in its complex is assumed to have Oh structure.

Electron spin resonance of copper complex

In this study the room temperature polycrystalline X-band ESR spectral pattern of [Cu L OH $(H_2O)_3$] complex, gave a similar spectral pattern. It is isotropic in nature where g_s=1.9339 with A=105 ($\times 10^{-4}cm^{-1}$). This behavior could be

explained depending on the donation of the oxygen atoms of the ligand hydroxy and water coordinating groups. Only one nitrogen atom coordinates [17-22].

Thermal analysis of red 2G and its complexes

Thermal analysis data of red 2G, Figures 1 and 5, gave series of decomposition steps according to weight loss as a function of temperature [23-25]. These steps appeared at T_{max} 60, 334, 454 and 562˚C, with activation energies Ea 53.56, 21.66, 570.37, 374.23 and 105.09 KJ mol^{-1}, Figure 6. The first one at T_{max}60ºC, is due to dehydration of the free ligand with activation energy Ea of 53.56KJ mol^{-1}, is exothermic step and considered as first order reaction. The second one at T_{max}163°C is due to elimination of two SO_3 molecules with low activation energy of 21.66 KJ mol^{-1}. This step is the fastest than the others. The reaction is of first order reaction. The third step at T_{max}334˚C the highest activation energy of 570.37KJ mol^{-1} is due to elimination of CH_3CONH_2 molecule in a first order reaction. Fourth step at T_{max} 454˚C with activation energy of 374 KJ mol^{-1}, is due to cleavage of organic compound in a second order reaction. The last step at T_{max} 562˚C, with activation energy 105.09 KJ mol^{-1} is due to breakdown of the complex and elimination of N_2H_4 molecule and formation of carbon as a final product. The values of collision numbers, Z, were 46.35, 10.56, 397.96, 339.29 and 85.04 S^{-1}, respectively. The values of the decomposed substance fraction, α_m=0.60, 0.63, 0.61, 0.45 and 0.44, respectively. The changes of entropy $\Delta S^{\#}$ values were -0.11, -0.12, -0.09, -0.09 and -0.11 kJ mol^{-1}, respectively. The changes in enthalpy $\Delta H^{\#}$ values were -39.08, -54.99, -58.25, -70.73 and -90.84 kJ mol^{-1}. β values were 2.26, 2.03, 2.26, 3.21 and 3.25, respectively, Figure 5.

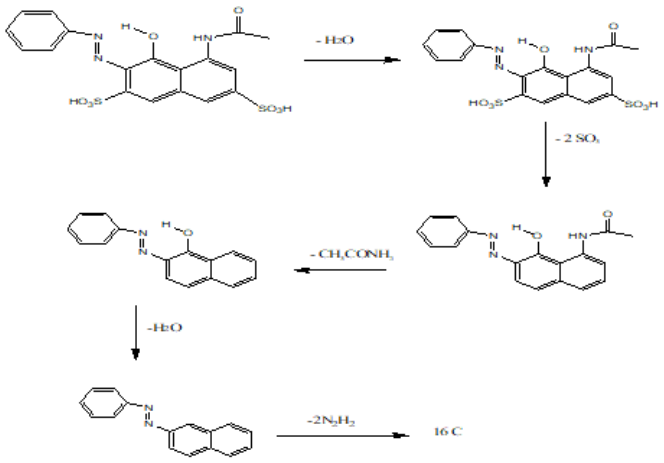

Figure 5. Thermal decomposition of Red 2G.

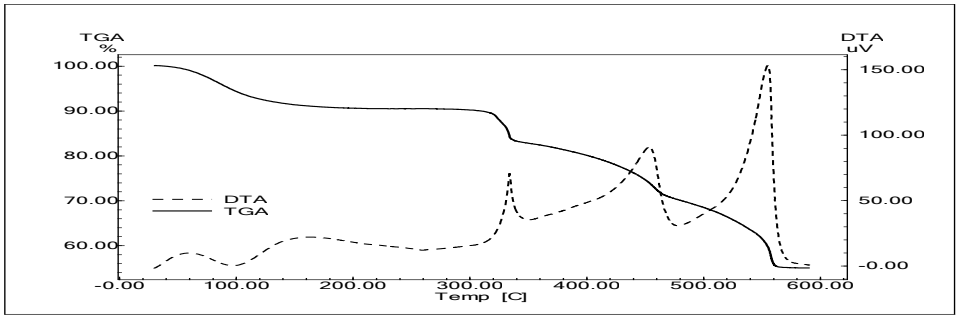

Figure 6. DTA and TGA of RED2G

The [Cr L $(OH)_2(H_2O)_2$] complex, Figures 7 and 8 and, showed four well defined peaks at 40, 153, 314 and 580°C from the DTA data, with activation energies of 63.25, 40.17, 229.02 and 44.08kJmole^{-1}. Their orders of reactions were first (n=0.99, 1.59, 1.22 and 0.912), respectively. All peaks are endothermic except the third one is exothermic in nature. However, the TGA data gave four peaks. The first is due to dehydration of $2H_2O$ and loss of two SO_3 molecules. The second one at T_{max} 153°C is due to loss of CH_3CONH_2, it is endothermic step with activation energy 40.17kJmole^{-1}, of first order reaction. The third step at T_{max} 314°C is due to breakdown of the complex and formation of $Cr(OH)_3$. This step is exothermic with high activation energy of 229.02 kJmole^{-1}. The increasing of activation energy indicates the low speed of the reaction at temperature range from 200 to 400°C. The fourth at T_{max} 580°Cwhich corresponding to decomposition of the complex and elimination of N_2H_4 molecules. Then formation of Cr_2O_3 and 14C as final products. The values of collision numbers, Z, were 33.09, 31.94, 119.99 and 11.31. Also, the values of the decomposed substance fraction, α_m=0.63, 0.54, 0.59 and 0.64, respectively. The changes of entropy $\Delta S^{\#}$ values were -0.12, -0.11, -0.10 and -0.12kJ mol^{-1}, respectively. The changes in enthalpy $\Delta H^{\#}$ values were -37.77, -50.44, -61.48 and -103.44 kJ mol^{-1}. β values were 1.26, 2.74, 2.36 and 1.80 respectively (Figure 7a).

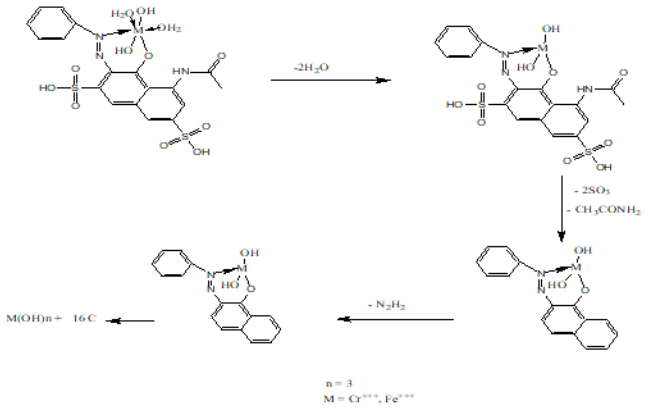

Figure 7a. Thermal decomposition of $Cr^{+++}$and Fe^{+++}Complexes of Red 2G.

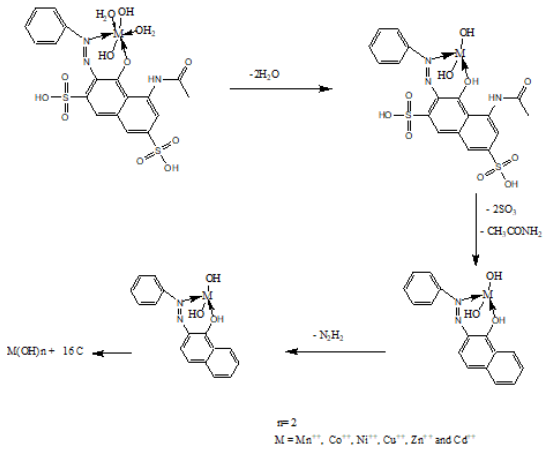

Figure 7b. Thermal decommission of Mn^{++}, Co^{++}, Ni^{++}, Cu^{++}, $Zn^{++}$and Cd^{++}Complexes of Red 2G.

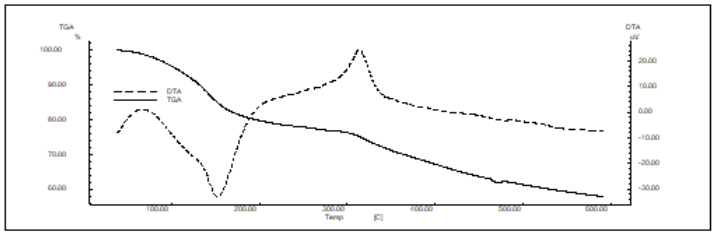

Figure 8. DTA and TGA of [Cr L $(OH)_2(H_2O)_2$].

The [Mn $LOH(H_2O)_3$] complex, Figure 9 and Table 2, showed four decomposition peaks at 62, 188.60, 327and 483°C from the DTA data, with activation energies of 34.58, 67.23, 292.25 and 109.25 $KJmole^{-1}$.All the steps considered as first order reaction except the last one is second order reaction, n=0.80, 0.98, 1.21and 1.93 respectively. All peaks are exothermic except the second one is endothermic in nature. The first peak is due to dehydration of coordinated and non-coordinated H_2O and loss of SO_3 molecule. The second one at T_{max}188.60°C is due to loss of CH_3CONH_2, it is endothermic step with activation energy 67.23 $kJmole^{-1}$, and is considered as first order reaction. The third step at T_{max} 327°C is due to breakdown of the complex and formation of $Mn(OH)_2$. This step is exothermic with high activation energy of 292.25$kJmole^{-1}$. The observed increasing of activation energy indicates the low speed of the reaction at temperature range from 160 to 245°C. The fourth at T_{max}483°C corresponds to decomposition of the complex and elimination of N_2H_4 molecule, then formation of MnO+14C as final products .The values of collision numbers, Z, were 19.33, 35.64, 151.60 and 52.71, respectively, and the values were α_m=0.63, 0.63, 0.59 and 0.50, respectively. The changes of entropy $\Delta S^{\#}$ values were -0.12, -0.11, -0.10 and -0.10kJ mol^{-1} respectively. The changes in enthalpy $\Delta H^{\#}$ values were -41.73, -53.92, -61.56 and -82.76 kJ mol^{-1}. β values were 1.50, 1.95, 2.34 and 2.96, respectively. Figure 7b.

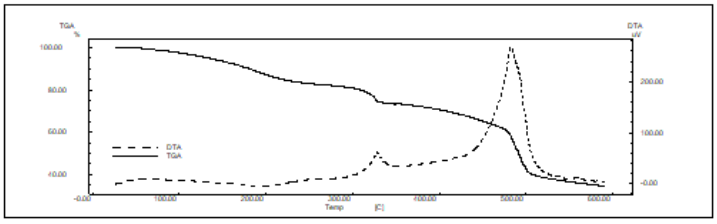

Figure 9. DTA and TGA of [Mn $LOH(H_2O)_3$].

The [Fe L^1 $(OH)_2(H_2O)_2$] complex, Figure 10, showed four well defined peaks from the DTA data at 160, 295, 375 and 500°C, with activation energies of 16.35, 241.37, 377.81 and 147.16 kJmole-1. Their orders of reactions were first (n=1.27, 1.26, 1.34 and 1.63), respectively. All peaks are exothermic in nature. However, the TGA data gave four peaks. The first is due to dehydration of $2H_2O$ and loss of two SO_3 molecules. The second one at T_{max}295°C is due to loss of CH_3CONH_2, of endothermic type with activation energy 241.37$kJmole^{-1}$, of first order reaction. The third step at T_{max}375°C is due to breakdown of the complex and formation of $Fe(OH)_3$, by exothermic type with high activation energy of 377.81 $kJmole^{-1}$. The observed increasing of activation energy indicates the low speed of the reaction. The fourth step at T_{max} 580°C which corresponding to decomposition of the complex and elimination of N_2H_2 molecule, then formation of Fe_2O_3+14C as final products. The values of collision number, Z, were 11.13,

134.92, 195.92 and 65.40 S-1, respectively. Also, the values of the decomposed substance fraction were α_m=0.58, 0.58, 0.57 and 0.53, respectively. The changes of entropy ΔS# values were -0.12, -0.10, -0.09and -0.10kJ mol^{-1}, respectively, and the changes in enthalpy ΔH# values were -55.00, -59.09, -64.69 and -83.09 kJ mol^{-1}. β values were 2.42, 2.41, 2.50 and 2.77, respectively, the mechanism of decomposition is represented in Figure 7a.

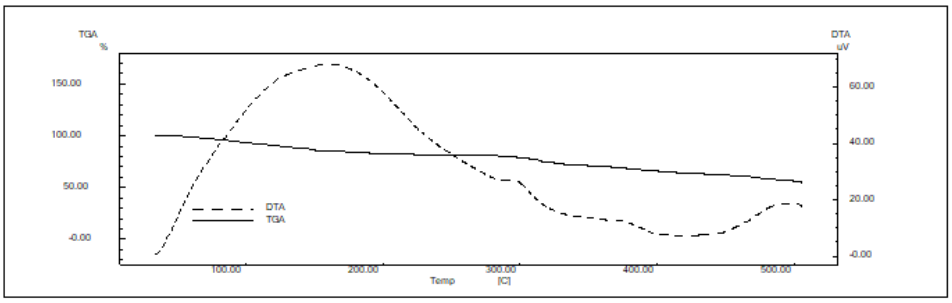

Figure 10. DTA and TGA of [Fe L^1 $(OH)_2(H_2O)_2$].

Similarly the [$CoLOH(H_2O)_3$] complex, Figure 11 and Table 2, the DTA curve data, gave four decomposition peaks at T_{max}100, 230, 310and 580°C, with activation energies of 42.19, 54.12, 192.56 and 84.97 $kJmole^{-1}$.All the steps are considered of first order reaction except the last one is second order type, (n=1.04, 1.15, 0.83and 1.99), respectively. All peaks are exothermic. The first peak at T_{max}100°C is due to dehydration of coordinated and non-coordinated H_2O and loss of SO_3 molecule. The second one at T_{max}230°C is due to loss of CH_3CONH_2, with activation energy 54.12$kJmole^{-1}$, this step is considered as first order reaction. The third step at T_{max} 310°C is due to breakdown of the complex and formation of $Co(OH)_2$. This step is exothermic type with high activation energy of 192.56$kJmole^{-1}$, the increasing of activation energy indicates the low speed of the reaction. The fourth at T_{max}580°C corresponds to decomposition of the complex and elimination of N_2H_4 molecule. Then the final products are CoO and carbon. The values of collision number, Z, were 29.30, 11.81, 67.39 and 36.39 S^{-1}, respectively. The values of the decomposed substance fraction wereα_m=(0.62, 0.60, 0.66 and 0.50), respectively. The entropy changes, $\Delta S^{\#}$, values were -0.12, -0.12, -0.10 and -0.11kJ mol^{-1}, respectively. The changes in enthalpy $\Delta H^{\#}$ values were -44.84, -3.02, -63.87 and -95.15 kJ mol^{-1}. β values were 2.07, 0.89, 1.59 and 2.57, respectively, Table 2, and the mechanism of decomposition is represented in Figure 7b.

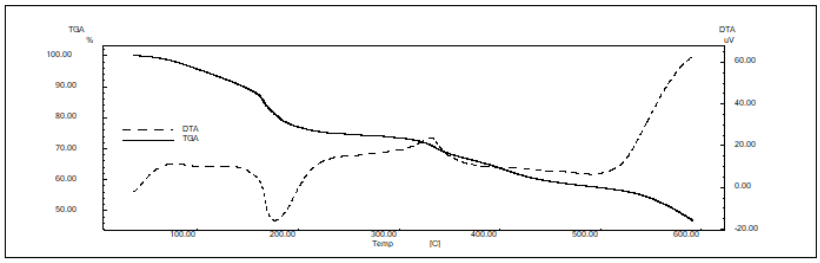

Figure 11. DTA and TGA of [Co $LOH(H_2O)_3$].

However the [Ni $LOH(H_2O)_3$] complex, Figure 12 and Table 2, showed four decomposition peaks at 70, 176, 331 and 600°C from the DTA data, with an activation energies of 23.07, 114.49, 119.64 and 89.46 $KJmole^{-1}$, respectively. All the steps considered of first order reaction were n=0.87, 1.27, 1.62 and 1.40, respectively. All peaks

are exothermic except the second one is endothermic in nature. The first peak at 70°C is due to dehydration of coordinated and non-coordinated H_2O molecule. The second one at T_{max} 176°C is due to loss of CH_3CONH_2 and SO_3, of endothermic type with activation energy 114.49KJmole^{-1}. This step is considered of first order reaction. The third one at T_{max} 331°C is due to breakdown of the complex and formation of $Ni(OH)_2$. This step is exothermic with activation energy of 119.64kJmole^{-1}. The fourth one appeared at T_{max}600°C which corresponding to decomposition and elimination of N_2H_4 molecule, then formation of NiO and C as final products.

The values of collision number, Z, were (14.09, 79.63, 68.53 and 32.14), respectively. Also, the values of the decomposed substance fraction, α_m=0.65, 0.58, 0.54 and 0.56, respectively. The changes of entropy $\Delta S^{\#}$ values were -0.12, -0.11, -0.10 and -0.11kJ mol^{-1}, respectively. The changes in enthalpy $\Delta H^{\#}$ values were -43.56, -49.56, -65.93 and -98.11 kJ mol^{-1}. β values were 1.70, 2.42, 2.76 and 2.57, respectively, Figure 7b.

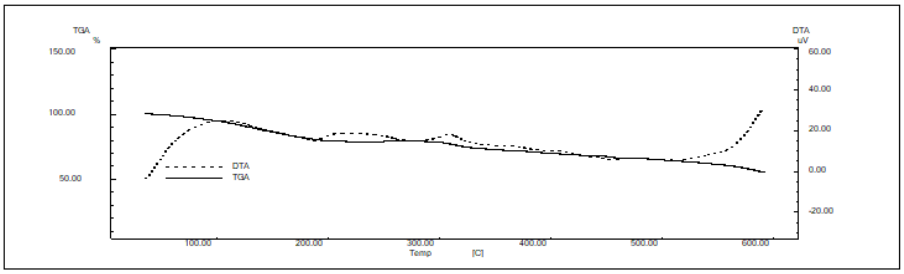

Figure 12. DTA and TGA of [Ni LOH(H_2O)$_3$].

However the [Cu LOH(H_2O)$_3$] complex, Figure 13 and Table 2, showed four decomposition peaks at 127, 261, 327 and 513°C, with activation energies 19.84, 145.33, 117.15 and 56.70 KJmole^{-1}, all the steps considered of first order reaction (n=1.33, 1.36, 1.15 and 1.78), respectively. All peaks are exothermic except the first one is endothermic in nature.

The first is due to dehydration of coordinated and non-coordinated H_2O and loss of SO_3 molecule with activation energy of 19.84 KJmol^{-1}. The second one at T_{max}261°C is due to loss of CH_3CONH_2 and SO_3, it is exothermic step with activation energy 145.33kJmole^{-1}. The third step at T_{max} 327°C is due to breakdown of the complex and formation of $Cu(OH)_2$, This step is exothermic with high activation energy of 117.15KJmole^{-1}, the observed increasing of activation energy indicates the low speed of the reaction. The fourth at T_{max}513°C corresponds to decomposition of the complex and elimination of N_2H_4 and H_2O molecules. Then the reaction is ended by formation of CuO+14C as final products.

The values of collision numbers, Z, were 15.12, 88.03, 55.21 and 25.23, respectively. Also, the values of the decomposed substance fraction wereα_m=0.57, 0.57, 0.60 and 0.52 S^{-1}, respectively. The changes of entropy $\Delta S^{\#}$ values were -0.12, -0.10, -0.11 and -0.11kJ mol^{-1}, respectively. The changes in enthalpy $\Delta H^{\#}$ values were -42.43, -54.31, -57.76 and -88.76 kJ mol^{-1}. β values were 2.27, 1.97, 2.41 and 1.39 respectively. The mechanism of decomposition is represented in Figure 7b.

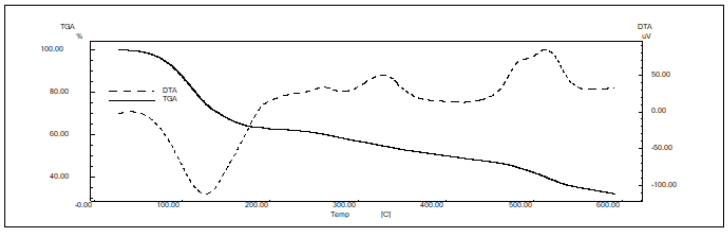

Figure 13. DTA and TGA of [Cu LOH(H_2O)$_3$].

The DTA of [Zn LOH(H_2O)$_3$] complex, Figure 14 and Table2, showed four decomposition peaks at 62, 163, 290 and 467°C with activation energies of 18.05, 26.77, 284.60 and 66.63 KJmole^{-1}. All the steps considered as first order reaction, n=1.16, 0.99, 1.26 and 0.99 respectively. All peaks are exothermic in nature. The first peak is due to dehydration of coordinated and non-coordinated H_2O molecules. The second one at T_{max} 163°C is due to loss of $CH_3CONH_2$and SO_3 molecules, with an activation energy 26.77kJmole^{-1}. The third step at T_{max} 290°C is due to breakdown of the complex and formation of $Zn(OH)_2$,This step is exothermic with high activation energy of 284.60 kJmole^{-1}, the increasing of activation energy indicates the slow rate of the reaction. The fourth at T_{max} 467°C corresponds to decomposition and elimination of N_2H_4 and H_2O molecules. Then formation of ZnO+14C as final products. The values of collision numbers, Z, were 15.03, 14.87, 163.41 and 15.27 S^{-1}, respectively. Also, the values of the decomposed substance fraction were α_m=0.60, 0.63, 0.58 and 0.63, respectively. The changes of entropy $\Delta S^{\#}$ values were -0.12, -0.12, -0.10 and -0.11kJ mol^{-1}, respectively. The changes in enthalpy $\Delta H^{\#}$ values were -42.43, -4.31, -57.71 and -88.76 kJ mol^{-1}. β values were 2.27, 1.97, 2.41 and 1.39, respectively. The mechanism of decomposition is represented in Figure 7b.

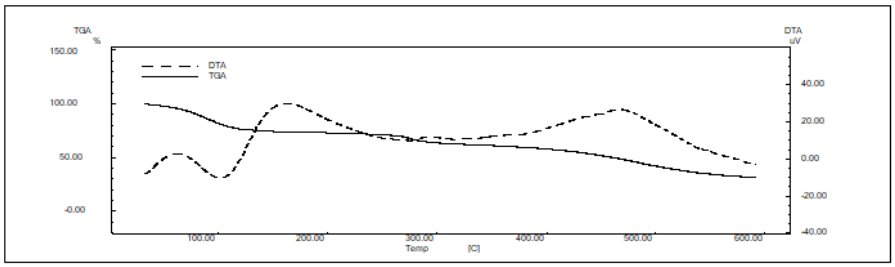

Figure 14. DTA and TGA of [Zn LOH(H_2O)$_3$].

For the [Cd LOH(H_2O)$_3$] complex, Figure 15 and Table 2,DTA showed four decomposition peaks at 159, 322, 441 and 507°C, with activation energies of 14.26, 265.31, 533.29 and 159.30 KJmole^{-1}. All the steps considered of first order type (n=1.29, 0.76, 1.26and 1.03), respectively. All peaks are exothermic in nature. The first peak is due to dehydration of coordinated and non-coordinated H_2O and loss of SO_3 molecule. The second one at T_{max}322°C is due to loss of CH_3CONH_2, and of exothermic type with activation energy 265.31KJmole^{-1}, this step is low speed because of it required high activation energy. The third step at T_{max}441°C is due to breakdown of the complex and formation of $Cd(OH)_2$. This step is exothermic with high activation energy of 533.29KJmole^{-1}. Fourth at T_{max}507°C is corresponding to decomposition and elimination of two $N_2H_4$and H_2O molecules, then, formation of CdO+14C as final products. The values of collision numbers, Z, were 8.32, 97.20, 390.28 and 83.56 S^{-1}, respectively. Also, the

values of the decomposed substance fraction wereα_m=0.58, 0.68, 0.58 and 0.62, respectively. The changes of entropy $\Delta S^{\#}$ values were -0.12, -0.10, -0.09and -0.10kJ mol^{-1}, respectively. The changes in enthalpy $\Delta H^{\#}$ values were -55.34, -64.07, -68.63 and -84.97 kJ mol^{-1}. β values were 2.44, 1.36, 2.41 and 2.05, respectively, Figure 7b.

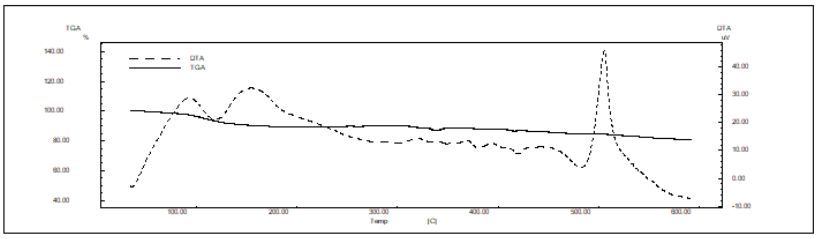

Figure 15. DTA and TGA of [Cd $L^1OH(H_2O)_3$].

Biological activity

Red 2G and its complexes showed activity to microorganisms in different ranges of cleration zones in neutrant agar media. The [Cr $L(OH)_2(H_2O)_2$] complex showed positive antibacterial action to Gram positive *Streptococcus* pyogenes with inhibition zone++, while *Staphylococcus Epidermidis*, Gram negative *E. coli and K. pneumonia* resist antimicrobial action [26-28]. The [Mn $LOH(H_2O)_3$] complex gave antibacterial activity to *Staphylococcus Epidermidis with inhibition zone++, where Streptococcus* pyogenes and Gram negative bacteria resist its biological activity. The [Fe $L(OH)_2(H_2O)_2$] complex showed biological activity to Gram positive *Streptococcus* pyogenes only with inhibition zone++. The [Co $LOH(H_2O)_3$] complex showed negative biological activity to *E. coli*and *K. pneumonia* and positive antimicrobial action to Gram positive *Streptococcus* pyogenes and *Staphylococcus Epidermidis* with inhibition zone+++and++, respectively.

Table 2. Antibacterial activity of Red2G and its complexes against some strains expressed in absolute activity.

Compound	Antibacterial activity			
	K. pneumoniae	***E. coli***	***S. pyogenes***	***Staph Epidermidis***
DMSO	-	-	+	+
Red 2G (HL)	-	-	-	+
[Cr $L(OH)_2(H_2O)_2$]	-	-	++	-
[Mn $LOH(H_2O)_3$]	-	-	-	++
[Fe $L(OH)_2(H_2O)_2$]	-	-	++	-
[Co $LOH(H_2O)_3$]	-	-	+++	++
[Ni $L OH(H_2O)_3$]	-	-	+	+
[Cu $L OH(H_2O)_3$]	-	-	-	+
[Zn $L OH(H_2O)_3$]	-	-	++	++

CONCLUSION

The [Ni $L OH(H_2O)_3$] showed antimicrobial activity in the same range of the solvent, its inhibition zones are 10 and 8 reflect its weak biological activity to screened microorganisms. The [Cu $L OH(H_2O)_3$] gave weak antimicrobial activity to *Staphylococcus epidermidis* with inhibition zone+, while it showed no biological activity with the other

microorganisms. The bacterial growth inhibition of the [Zn $LOH(H_2O)_3$] complex to gram positive bacteria refers to the highly biological activity of zinc compounds.

REFERENCES

1. RH Lee, E Griswold, J Kleinberg. *Inorg Chem.* **1964,** 3(9), 1278.
2. MS Masoud, HA Motaweh, AE Ali. *Indian J Chem*. **2001**, 40, 733.
3. MS Masoud, Alaa E Ali, Hytham M Ahmed, Essam A Mohamed. J Molecular Structure. **2013**, 43, 1050.
4. MS Masoud, SA Abou El-Enein, IM Abed, AE Ali. *J Coord Chem*. **2002**, 55(2), 153.
5. MS Masoud, AE Ali, GS Elasala, SA kolkaila. *Spectrochim Acta*. **2018**, 193, 458-466.
6. MS Masoud, AE Ali, GS Elasala, S Akolkaila. *J Chem Pharm Res.* **2017**, 9, 171-179.
7. TM Salem, RM Issa, MS Masoud. *Egypt J Chem*. **1973**, 16(4), 283-295.
8. AE Ali, GS Elasala, EA Mohamed, SA kolkaila. *Heliyon*. **2019**, 5(11).
9. S Hedewy, SK Hoffman, MS Masoud, J Goslar. *SpectrLett.* **1986,** 9, 917.
10. MS Masoud, TM Salem, FM Ashmawy. *Revue Roumaine de chimie*. **1978**, 23(9-10), 1367-1372.
11. ER Price, JR Wasson. *J Inorg Nucl Chem*. **1974**, 36(1), 67.
12. ABP Lever, D Ogden. *J Chem Soc A*. **1967**, 2041.
13. FA Cotton. *Wiley Eastern Limited, London.***1979.**
14. KD Karlin, J Zubieta. *Adenine Press, New York.***1983**.
15. S Hedewy, SK Hoffman, MS Masoud, J Goslar. *Spectr Lett*. **1986**, 19, 917.
16. L Que. *University Science Books, Sausalito, California*. **2000**.
17. MS Masoud, MF Amira, AM Ramadan, GM El-Ashry. *Spectrochim ActaA*. **2008**, 69, 230.
18. MS Masoud, EA Khalil, AM Hafez, AF El-Husseiny. *Spectrochim Acta*. **2005**, 61A, 989.
19. MS Masoud, EA Khalil, AM Hindawy, AE Ali, EF Fawzy. *Spectrochim Acta*. **2004**, 60A, 2807.
20. MSMasoud, MM El-Essawi. *J Chem Eng Data*. **1984**, 29, 363.
21. MS Masoud, AM Hafez, AE Ali. *Spectrosc Lett*. **1998**, 31(5), 901.
22. MS Masoud. *Metal-Organic, Nano-Metal Chemistry*. **2010**, 40, 1.
23. HE Kissinger. *Anal Chem*. **1957**, 29(11), 1702.
24. K Traore. *J Therm Anal.* **1972**, 4(2), 135.
25. GO Piloyan, ID Ryabchikov, OS Novikova. *Nature*. **1966**, 1229.
26. N Raman, A Kulandaisamy, C Thangaraja, P Manisankar, S Viswanathan, C Vedhi. *Trans Met Chem*. **2004**, 29(2), 129.
27. E Canpolat, M Kaya, S Gür. *Turk J Chem*.**2004**, 28, 235-242.
28. SJ Kirubavathy, R Velmurugan, K Parameswari, S Chitra. *IJPSR*. **2014**, 5(6), 2508.